

Isothermal Crystallization of HDPE/Octamethyl Polyhedral Oligomeric Silsesquioxane Nanocomposites: Role of POSS as a Nanofiller

M. Joshi, B. S. Butola

Department of Textile Technology, Indian Institute of Technology, New Delhi 110016, India

Received 25 June 2007; accepted 14 November 2007

DOI 10.1002/app.26318

Published online 6 April 2007 in Wiley InterScience (www.interscience.wiley.com).

ABSTRACT: The isothermal crystallization of HDPE/POSS (polyhedral oligomeric silsesquioxane) nanocomposites (POSS content varying from 0.25 to 10 wt %) was studied using differential scanning calorimetry (DSC) technique. The Avrami model could successfully describe the isothermal crystallization behavior of the nanocomposites. The value of Avrami exponent (n) varies between 2 and 2.5 for all the compositions studied. For a given composition, the values vary with crystallization temperature and in general increased with POSS content up to 1 wt % POSS content and decreased thereafter. The presence of POSS was found to increase the rate of crystallization, which manifested itself in the increased value of the Avrami rate constant (K) and

reduced value of crystallization half-time ($t_{1/2}$). The rate of crystallization peaked at 1 wt % POSS content and was almost constant at higher POSS loadings. X-ray diffraction studies revealed that POSS exists as nanocrystals in HDPE matrix while some POSS gets dispersed at molecular level too. It is observed that only the POSS dispersed at molecular level acts as a nucleating agent while the POSS nanocrystals do not affect the crystallization process. © 2007 Wiley Periodicals, Inc. *J Appl Polym Sci* 105: 978–985, 2007

Key words: polyhedral oligomeric silsesquioxane; nanocomposites; isothermal crystallization; X-ray diffraction; Avrami analysis

INTRODUCTION

The presence of additives and fillers significantly affects the crystallization kinetics of polymers and is well documented, but there are rather few studies describing the effect of nanoparticles on crystallization behavior^{1–4} of the polymeric matrix in nanocomposites. A nanoparticle is different from a conventional additive/filler in two respects: first, because of its very small size, it is capable of entering into molecular level interactions with the polymeric chains and second, it can introduce very high surface areas into the matrix because of its high aspect ratios. These studies assume importance in the light of polymeric nanocomposites attracting a lot of interest lately and having potential for use in high performance technical and engineering applications. They combine the advantages of improvement in performance properties such as strength/modulus, gas barrier, flame retardancy, thermal stability, etc., at low filler content along with being lightweight.

Polyhedral oligomeric silsesquioxanes (POSS) (Fig. 1) can be considered as a new class of nanofillers, which have been used for the synthesis of a range of poly-

meric nanocomposites in the last decade.^{5–10} Its size (~1 nm) is among the smallest of all the nanostructured materials available today. In most of these nanocomposites, the POSS moiety is covalently bonded with the main chain. However, there are fewer studies^{11,12} where POSS is physically blended with polymers for preparation of polymeric nanocomposites. In the previous study, the authors have described the nonisothermal crystallization behavior of POSS–HDPE nanocomposites.¹³ This study describes the isothermal crystallization kinetics of HDPE/POSS polymeric nanocomposites.

EXPERIMENTAL

Materials

The HDPE used in the study was supplied by Reliance Industries Limited, India (Relene E 52,009—Oriented Tape and monofilament grade) with an MFI of 0.9. The POSS used was Octamethyl POSS (MS 0830, where R—CH₃) supplied by Hybridplastics, Fountain Valley, USA.

Nanocomposite preparation

The masterbatch of POSS in HDPE (10 wt % loading) was prepared on a twin-screw extruder (APV Baker, model—MP 19 TC) by melt mixing. The processing

Correspondence to: M. Joshi (mangala@textile.iitd.ernet.in).

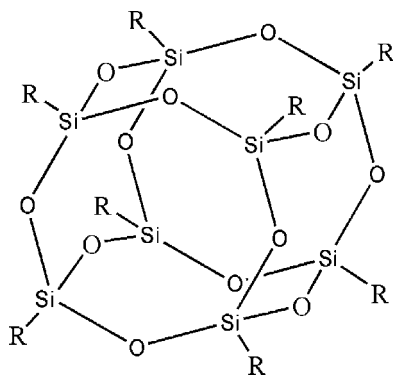


Figure 1 Molecular structure of POSS (R- any organic group).

conditions are given in Table I. The 10 wt % POSS masterbatch was then used to prepare HDPE/POSS nanocomposites of various compositions, the details of which are given in Table II.

The nanocomposite filaments were prepared by melt extrusion of HDPE and the masterbatch in suitable ratios to get the above-mentioned compositions in the laboratory single screw extruder (Betol, UK). The different barrel zone temperatures were 210, 230, and 250°C, respectively, and the die temperature was kept at 270°C. The take-up speed was maintained at 12 m/min and the extrudate was solidified by quenching it in a water bath maintained at 12–14°C.

Crystallization study

The crystallization behavior was studied on a Perkin-Elmer Pyris-1 series DSC seven differential scanning calorimeter under a flowing nitrogen atmosphere. The sample weight was kept around 5 mg for all the tests. The isothermal crystallization tests were carried out at 118, 119, 120, and 121°C. The samples were heated to 180°C at a heating rate of 20°C/min and held for 5 min to erase any thermal history. The samples were then cooled at the rate of 150°C/min to the crystallization temperatures (T_c) and held at that temperature till the crystallization was complete.

X-ray diffraction studies

The determination of volume fraction crystallinity and crystallite size was done by carrying out wide

TABLE I
Processing Conditions for Melt Mixing of POSS and HDPE in Twin Screw Extruder

Barrel zone temperatures (°C)	165, 185, 215, 225
Die zone temperature (°C)	240
Screw RPM	60

TABLE II
Composition of Various HDPE-POSS Nanocomposites

POSS content (wt %)	HDPE content (wt %)	Nanocomposite code
0.0	100.0	HDPE
0.25	99.75	P025
1.0	99.0	P1
3.0	97.0	P3
5.0	95.0	P5
10.0	90.0	P10

angle X-ray diffraction (WAXD) of the samples on a Philips X-ray diffractometer with nickel-filtered Cu K α (1.54 Å) as radiation source. The diffractometer was operated at 40 kV and 30 mA in reflection mode with angle 2θ range 10° to 40° at a scanning rate of 2°/min. The characterization of neat POSS and POSS crystallites in HDPE was carried out on a Bruker AXS X-ray diffractometer (D8 Advanced) using Cu K α radiation operated at 40 kV and 30 mA. The data were collected in 2θ angle range 2° to 35° at a scanning rate of 0.5°/min.

Transmission electron microscopy

The dispersion of POSS in HDPE at finer level was studied on a FEI Technai F20 field emission TEM operating at an accelerating voltage of 200 kV. The samples were prepared by cutting thin sections of selected HDPE-POSS nanocomposite monofilaments with a Microtome-Ultracut-E Reichert Jung ultramicrotome in cryogenic conditions.

RESULTS AND DISCUSSION

Isothermal crystallization kinetics

Figure 2 shows the typical DSC curves of heat flow as a function of temperature at different cooling rates for neat HDPE and HDPE/POSS nanocomposite (99 : 1). The determination of the absolute crystallinity is not required for the analysis of crystallization kinetics. It can be done by determining the relative degree of crystallinity $X(t)$ as a function of time at a constant temperature. The relative crystallinity can be defined as

$$X(t) = Q_t/Q_\infty = \frac{\int_0^t (dH/dt)dt}{\int_0^\infty (dH/dt)dt} \quad (1)$$

where Q_t and Q_∞ are the heat evolved at time t and infinite time, respectively, and dH_c/dT is the heat flow rate.

The development of relative crystallinity with time for HDPE and POSS-HDPE nanocomposites at different crystallization temperatures is plotted in Figure 3.

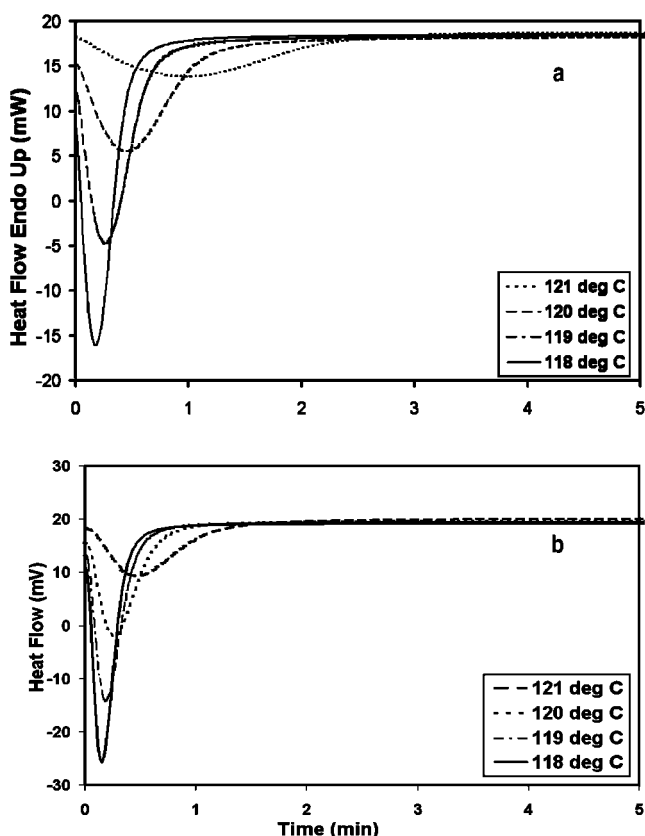


Figure 2 Crystallization isotherms of HDPE and HDPE-POSS nanocomposites at different crystallization temperatures (a) HDPE and (b) P1.

Avrami analysis

The analysis of the time-dependent relative crystallinity function $X(t)$ for isothermal crystallization process was carried out using Avrami equation¹⁴⁻¹⁶ as described below:

$$X(t) = 1 - \exp(-Kt^n) \quad (2)$$

The above equation can be rearranged as follows by taking its double logarithm

$$\log[-\ln(1 - X(t))] = n \log t + \log K \quad (3)$$

where n , the Avrami exponent is a mechanism constant, which depends on the type of nucleation and growth process, K is the Avrami rate constant involving nucleation and growth parameters, and t is the crystallization time. According to original assumptions of the theory, the value of the Avrami exponent n should be an integer ranging from 1 to 4.

If the eq. (3) adequately describes the isothermal crystallization kinetics of a polymer then the plots of $\log[-\ln(1 - X(t))]$ and $\log t$ would be straight lines and one should be able to obtain the values of n and K from the slopes and the intercepts, respectively. The Avrami plots of $\log[-\ln(1 - X(t))]$ versus $\log t$

for HDPE and HDPE-POSS nanocomposites are shown in Figure 4. It is clear that except for the initial nonlinear part of the plots, which signifies induction or seeding phase of crystallization, most of them are fairly linear. Hence, it can be assumed that Avrami model is able to satisfactorily describe the isothermal crystallization kinetics of HDPE and HDPE-POSS nanocomposites. The values of Avrami parameters n , K , and crystallization half-time $t_{1/2}$ (determined from Fig. 3) were determined from the linear portions of the curves and are given in Table III. The values of Avrami exponent n for HDPE, P025, P1, P3, P5, and P10 range from 2.06 to 2.26, 2.13 to 2.49, 2.21 to 2.52, 2.14 to 2.43, 2.10 to 2.35, and 2.2 to 2.43, respectively. From the data, it is clear that the values of n for HDPE and all nanocomposites lie between two and three.

Generally, the values of n reported for polyethylene in the literature¹⁷⁻²¹ range from two to four, mostly for isothermal crystallization. These values have been interpreted in terms of simultaneous occurrence of tridimensional (spherulitic) growth from heterogeneous ($n = 3$) and homogeneous ($n = 4$) nuclei. However, the values reported by Chang and coworkers²² lie below two, reducing significantly from 1.74 at crystallization temperature of 122°C to 1.07 at 117°C. The variation in the values

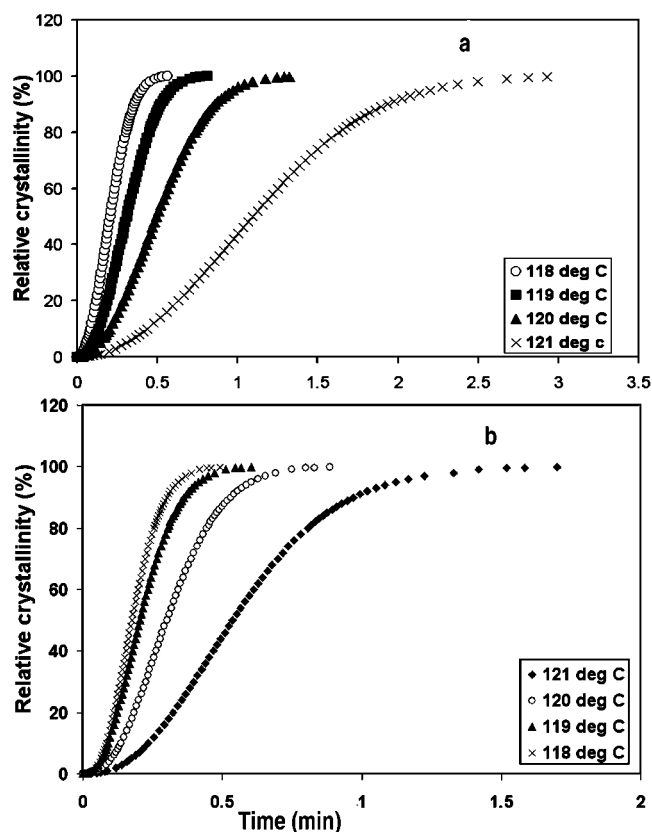


Figure 3 Development of relative crystallinity with crystallization time for (a) HDPE and (b) P1.

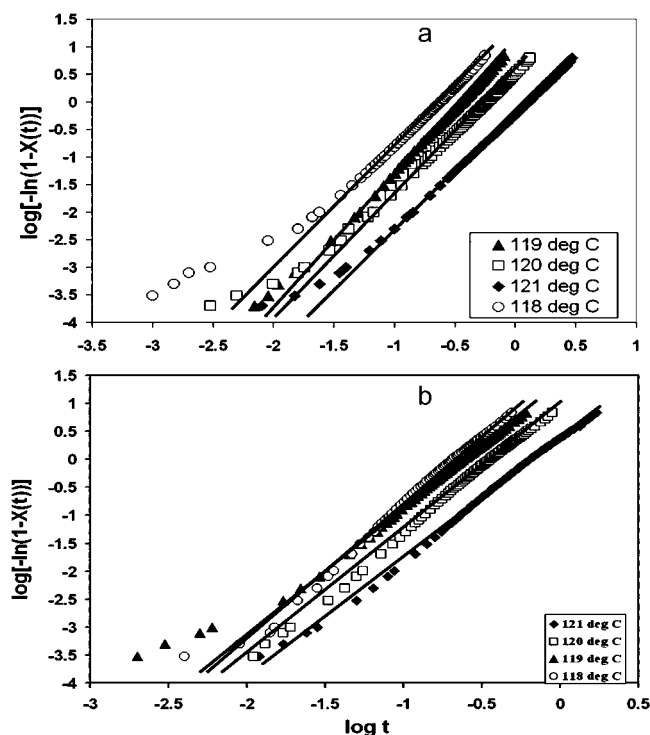


Figure 4 Plots of $\log[-\ln(1 - X(t))]$ versus $\log t$ for isothermal crystallization of (a) HDPE and (b) P1.

was explained on the basis of occurrence of recrystallization or reorganization processes.^{23–25}

The average values of n for HDPE and HDPE–POSS nanocomposites at the four crystallization temperatures (118, 119, 120, and 121°C) has been computed and used in further analysis. The values of n range from 2.04 to 2.52 for HDPE and different POSS/HDPE nanocomposites, which are in agreement with the literature values. Figure 5 shows variation of Avrami constant n with POSS content at different crystallization temperatures. It is clear that the values of n reach a maximum at 1 wt % POSS content and then reduces gradually with further increase in POSS content. This

is in contrast to the study by Fornes and Paul²⁶ who reported a systematic decrease in the value of n with increase in organoclay content in nylon 6 and Hirai and coworkers³ who also observed decrease in the value of n for silica nanoparticle in PEN matrix for the case of nonisothermal crystallization.

A look at the values of n reported by different researchers indicates that the values of n are sensitive to the type of filler and the polymer (in terms of the degree of short- and long-chain branching) that has a strong influence on the extent to which the polymer can crystallize. Hence, the values of n may not be comparable for different systems. The values of n ranging from 2.04 to 2.52 for HDPE and different POSS/HDPE nanocomposites suggest the following possibilities:

1. simultaneous occurrence of two and three dimensional crystal growth with heterogeneous nucleation;
2. simultaneous occurrence of two dimensional crystal growth with heterogeneous and homogeneous nucleation;
3. combination of the above two mechanisms.

It is postulated that the lower values of n (close to 2) at 0.25 wt % POSS is due to the dominance of two-dimensional crystallization with heterogeneous nucleation. However, with increase in POSS concentration around 1 wt %, three-dimensional crystallization with heterogeneous nucleation also starts dominating, which pushes the value of n towards 2.5. Further increase in POSS concentration does not change the value of n significantly; as POSS starts forming crystalline aggregates as is evident from X-ray diffraction analysis discussed below and these do not contribute towards heterogeneous nucleation and a three-dimensional crystallization.

The values of Avrami parameter, K varies between 1.05 and 50.12. It is interesting to note that at each

TABLE III
Kinetic Parameters for HDPE and POSS–HDPE Nanocomposites from the Avrami Analysis

Temperature	Crystallization parameters (°C)	HDPE	P025	P1	P3	P5	P10
121	n	2.04	2.13	2.21	2.14	2.14	2.2
	$\log K$	0.23	0.02	0.40	0.36	0.34	0.37
	$t_{1/2}$	1.094	0.81	0.537	0.553	0.563	0.554
120	n	2.15	2.15	2.33	2.24	2.12	2.2
	$\log K$	0.50	0.76	1.02	0.83	0.86	0.86
	$t_{1/2}$	0.497	0.375	0.301	0.35	0.322	0.337
119	n	2.33	2.4	2.22	2.3	2.10	2.2
	$\log K$	1.03	1.24	1.34	1.22	1.22	1.22
	$t_{1/2}$	0.309	0.258	0.205	0.244	0.215	0.231
118	n	2.06	2.49	2.52	2.43	2.35	2.46
	$\log K$	1.27	1.56	1.7	1.52	1.57	1.57
	$t_{1/2}$	0.206	0.2	0.175	0.197	0.178	0.191

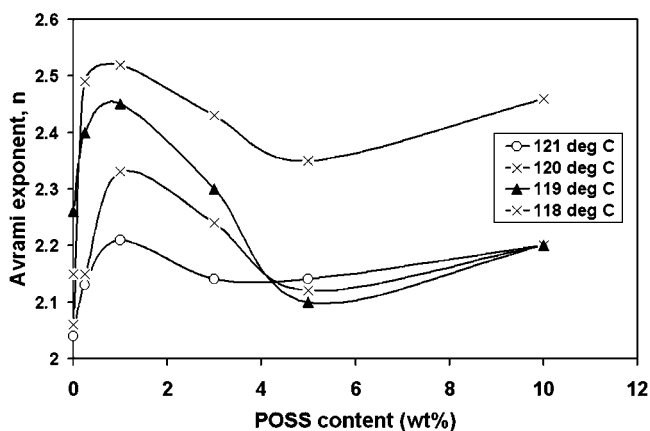


Figure 5 Variation of Avrami exponent, n with POSS content in HDPE.

crystallization temperature studied, the value of K first increases with increase in POSS content, reaches a maximum at 1 wt % POSS, drops, and remains fairly constant between 3 and 10 wt % POSS. That means that the plots of K and POSS content at different temperature show a peak at 1 wt % POSS (Fig. 6). Since K is related with rate of crystallization, this means POSS definitely plays a role in increasing the rate of crystallization by acting as effective heterogeneous nucleating sites. At low concentrations (below 1 wt %), POSS remains uniformly distributed at nano or molecular level in HDPE matrix as also supported by TEM study. In this form, POSS macromers act as effective nucleation sites and increase the crystallization rate. The maximum nucleation activity is shown at 1 wt % POSS content, as at this concentration maximum amount of POSS remains distributed in HDPE matrix at nano/molecular level uniformly. Further increase in POSS concentration merely results in increase in level of POSS agglomerates (loosely held network of small POSS crystallites). These agglomerates do not contribute towards nucleation activity and hence rate of crystallization does not change much between 3 and 10 wt % POSS content. In fact, the amount of uniformly distributed POSS macromers may drop slightly beyond 1 wt % POSS concentration, which accounts for a drop in rate of crystallization. Hence, it can be concluded that only the POSS dispersed at the molecular/nano-level affects the crystallization mechanism as well as the rate of crystallization of HDPE matrix by contributing as a heterogeneous nucleating agent under isothermal crystallization conditions.

The value of K is very sensitive to the crystallization temperature and increases sharply with decrease in crystallization temperature. This creates a practical difficulty in the selection of temperature range for determination of isothermal crystallization rates and has also been discussed elsewhere.²¹ The variation of Avrami parameter K with POSS content

shows a maxima at 1 wt % POSS content, similar to the relation between Avrami exponent, n , and POSS content. This trend is similar to the one reported by Fornes and Paul, who report that higher clay loadings impede crystallization of nylon 6. Contrary to this, Chang and coworkers²² observed that crystallization rates go down at low clay content in PE and increase with increase in clay content but always remain lower than pristine PE. According to them, clay enhances the crystallization rate only at higher clay loading when it aggregates and acts as a nucleating agent. This seems to be in sharp contrast to the observation of Fornes and Paul²⁶ who reported reduction in crystallization rates above 0.9 wt % clay. The reason may lie in the fact that the mode of interaction of nanofillers with the polymeric matrix is significantly affected by the type of polymer and the nanofiller.

The crystallization half-time ($t_{1/2}$) decreases for all nanocomposites when compared with neat HDPE. It is minimal for 1 wt % sample and then increases slightly from 3 to 10 wt % POSS samples. This is to be expected since constant K , which indicates the rate of crystallization is maximum at 1 wt % POSS content and decreases thereafter.

X-ray scattering studies

The weight fraction crystallinity of the nanocomposite filaments was determined by superimposing the amorphous curve on the $I(\theta)$ vs. θ diffraction scans obtained from the X-ray diffractometer and using the following formula after segregating the crystalline contribution:

$$X_c = \frac{\int_0^\alpha s^2 I_c(s) ds}{\int_0^\alpha s^2 I_s(s) ds} \quad (4)$$

where X_c is the crystalline mass fraction, $S = 2 \sin \theta / \lambda$, I_c the crystalline diffraction intensity, I_s the total dif-

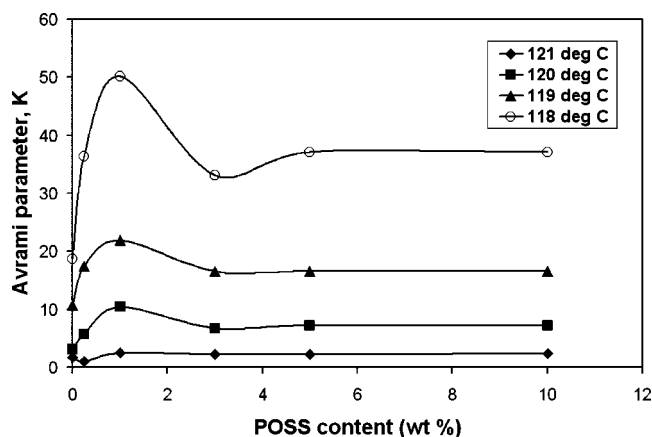


Figure 6 Variation of Avrami parameter, K with POSS content in HDPE.

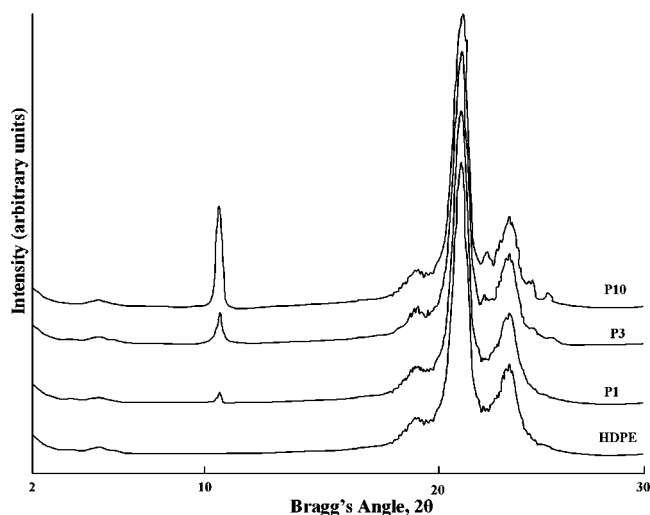


Figure 7 XRD diffractograms of HDPE and HDPE-POSS nanocomposites.

fraction intensity, $\lambda = 1.54 \text{ \AA}$, and θ the Bragg's angle.

The average lateral crystalline thickness is estimated from the broadening observed in the WAXD pattern recorded for 2θ range of 10° – 35° at a scanning rate of $2^\circ/\text{min}$. The integral breadth of the diffraction intensity arising from the imperfection of crystallites is measured in terms of $\beta_{[1/2]}(hkl)$. Higher the value of $\beta_{[1/2]}(hkl)$, lower is the crystalline perfection.

Apparent crystalline size was determined according to Scherrer's equation:

$$D(hkl) = \frac{K\lambda}{\beta \cos \theta} \quad (5)$$

where β is the half width of the diffraction peak in radian, K is equal to 0.9, θ is the Bragg angle, and λ is the wave length of the X-rays. The values of D_{hkl} for (110) reflection were calculated.

The X-ray diffraction patterns of selected HDPE-POSS nanocomposites are shown in Figure 7. It is clear that POSS exists as crystals in HDPE matrix, as the diffraction peak characteristic of POSS crystalline form ($\sim 10^\circ$) is observed in all nanocomposites samples. This is to be expected since POSS is reported⁵ to crystallize even when it is a part of the polymer chain and there are severe restrictions on its movement. It is further seen that POSS can retain its crystalline structure in EP copolymer matrix even at a temperature of 200°C , as reported in a recent study by Fu et al.¹² Therefore, it is obvious that in this study, some POSS exists in a crystalline state, since the experiments were carried out at much lower room temperatures. Another observation that can be made from the diffractograms is that the POSS peaks in nanocomposites are not as sharp as neat POSS

peaks indicating that these dispersed POSS crystals are not as perfect as the neat POSS crystals. It can also be inferred that, although the process of melt mixing disperses POSS at nano/molecular level in HDPE matrix, at lower concentrations, POSS eventually tends to crystallize and form agglomerates when concentration levels increases beyond 1 wt %. The size of the POSS crystals was determined using Scherrer's equation and given in Table IV. It is clear from the results that crystals from dispersed POSS in nanocomposites are smaller than that of the neat POSS crystals.

The X-ray diffractograms in Figure 7 show a gradual increase in the intensity of the diffraction peak characteristic of POSS ($\sim 10^\circ$). Although at 0.25 wt %, a very low POSS content at this peak is absent (not shown in the figure), but the crystallization rate constant shows an increase when compared with pristine HDPE. Absence of the diffraction peak at 0.25% POSS content leads us to believe that the POSS is distributed uniformly in HDPE matrix at nanolevel and though there may be a very few POSS aggregates/crystallites present, it may not be discernible in X-ray diffractograms due to very low concentration. The increase in crystallization rate constant is assumed to be because of the uniformly dispersed POSS macromers at molecular or nanolevel in HDPE matrix acting as nucleating agents. When the POSS content in HDPE is increased beyond 1%, POSS starts to form agglomerates and the concentration of uniformly dispersed POSS in HDPE at nanolevel decreases slightly. This accounts for a drop in Avrami rate constant. The POSS crystalline aggregates do not exhibit any nucleation activity and hence the Avrami parameter K remains almost constant between 3 and 10 wt % POSS content.

Transmission electron microscopy studies

Transmission electron micrographs of ultramicrotomed sections of neat HDPE and selected HDPE-POSS nanocomposites under cryogenic conditions are given in Figure 8. The images show comparatively uniform and homogeneous phase dispersion of POSS in HDPE matrix at 1 wt % POSS. This indicates disintegration of POSS particles because of shear during mixing and POSS getting dispersed in HDPE at molecular/nanolevel. It may be mentioned

TABLE IV
Crystal Size of POSS in Free and Dispersed State
(Using Sherrer's Equation)

Material	Crystal size (nm)
Neat POSS	40
P3	25
P10	25

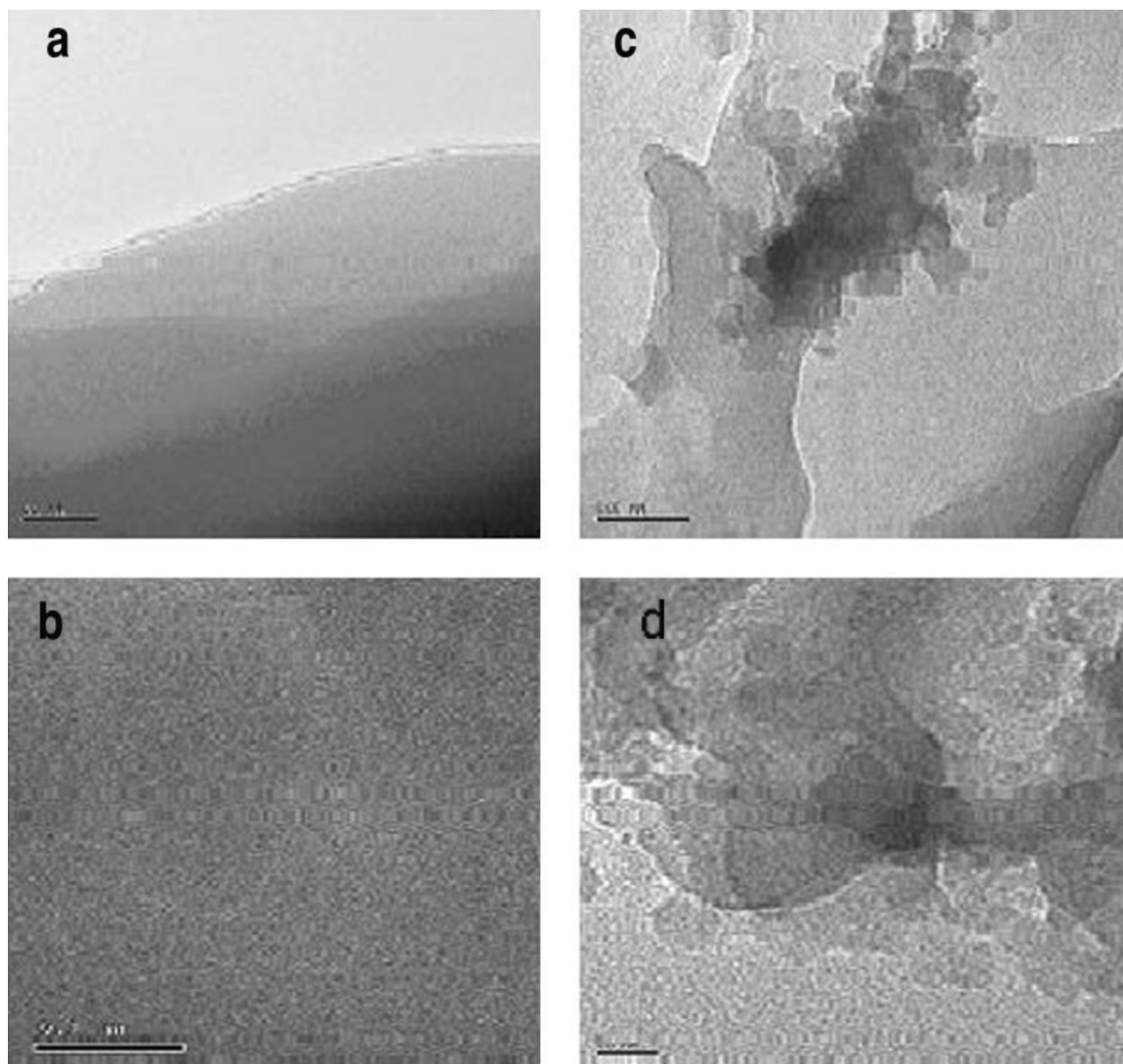


Figure 8 Transmission electron microscopy images of HDPE and selected HDPE-POSS nanocomposites (a), HDPE (b), P1 (c), and (d) P10.

here that since POSS macromers are particulate in nature, they may not be clearly discernible in TEM images such as nanoclay platelets or nanofibers. However, at 10 wt % POSS, agglomerates of POSS or darker POSS rich regions can be observed, which are seen different from the HDPE matrix. The actual size of these regions is much higher than 25 nm, as determined from X-ray studies. It is further suggested that these POSS nanocrystals may form a loosely held three-dimensional network at POSS concentrations between 5 and 10 wt %, which may give rise to gelation or solidlike behavior in nanocomposite melts as discussed in an earlier work²⁷ by the authors.

The study of rheological behavior of POSS-HDPE nanocomposites described by the authors²⁷ also support the miscibility (or uniform dispersion) of POSS in HDPE matrix at low concentrations (up to 1 wt %) and phase separation (or agglomeration) at higher concentrations (5 and 10 wt %).

CONCLUSIONS

The isothermal crystallization kinetics of HDPE and HDPE-POSS nanocomposites follow the Avrami model. The Avrami plots of HDPE and HDPE/POSS nanocomposites show linear trend, indicating the

applicability of Avrami model to describe the isothermal crystallization behavior of HDPE and HDPE-POSS nanocomposite systems. The value of Avrami exponent, n varied between 2 and 2.5 for all the systems studied and did not show a strong dependence on temperature. Average “ n ” value increases with increase in POSS content, reaches a maximum at 1 wt %, and then decreases but is always higher than that for neat HDPE.

The variation of Avrami parameter, K showed a similar trend. However, the “ K ” values were almost constant for POSS concentrations higher than 1 wt %. The crystallization half-time ($t_{1/2}$) decreases for all nanocomposites when compared with neat HDPE. It is minimal for 1 wt % sample and then increases slightly for 3–10 wt % POSS samples. POSS disperses uniformly at nanolevel in HDPE matrix up to 1 wt % content, and starts to agglomerate forming POSS crystals beyond 1 wt % concentration. The molecularly dispersed POSS acts as a nucleating agent whereas the crystalline POSS aggregates do not contribute towards nucleation activity. Thus, only the POSS dispersed at the molecular level affects the crystallization mechanism as well as the rate of crystallization of the HDPE matrix under isothermal crystallization conditions by acting as a heterogeneous nucleating agent.

The authors wish to thankfully acknowledge Dr. T. McNally, School of Material Sciences, Queen's University, Belfast, UK for his help in carrying out TEM analysis for this study.

References

1. Bogoeva-Gaceva, G.; Janevski, A.; Mader, E. *Polymer* 2001, 42, 4409.
2. Mucha, M.; Marszalek, J.; Fidrych, A. *Polymer* 2000, 41, 4137.
3. Kim, S. H.; Ahn, S. H.; Hirai, T. *Polymer* 2003, 44, 5625.
4. Li, J.; Zhou, C.; Gang, W. *Polym Test* 2003, 22, 217.
5. Zheng, L.; Waddon, A. J.; Farris, R. J.; Coughlin, E. B. *Macromolecules* 2002, 35, 2375.
6. Mather, P. T.; Jeon, H. G.; Romo-Urbe, A.; Haddad, T. S.; Lichtenhan, J. D. *Macromolecules* 1999, 32, 1194.
7. Romo-Urbe, A.; Mather, P. T.; Haddad, T. S.; Lichtenhan, J. D. *J Polym Sci Part B: Polym Phys* 1998, 36, 1857.
8. Mantz, R. A.; Jones, P. F.; Chaffee, K. P.; Lichtenhan, J. D.; Gilman, J. W.; Ismail, I. M. K.; Burmeister, M. *J Chem Mater* 1996, 8, 1250.
9. Hong, B.; Thoms, T. P. S.; Murfee, H. J.; Lebrun, M. *J Inorg Chem* 1997, 36, 6146.
10. Zhang, C.; Babonneau, F.; Bonhomme, C.; Laine, R. M.; Soles, C. L.; Hristov, H. A.; Yee, A. F. *J Am Chem Soc* 1998, 120, 8380.
11. Haddad, T. S.; Lichtenhan, J. D. *Macromolecules* 1996, 29, 7302.
12. Fu, B. X.; Gelfer, M. Y.; Hsiao, B. S.; Phillips, S.; Viers, B.; Blansku, R.; Ruth, P. *Polymer* 2003, 44, 1499.
13. Joshi, M.; Butola, B. S. *Polymer* 2004, 45, 4953.
14. Avrami, M. J. *J Chem Phys* 1939, 7, 1103.
15. Avrami, M. J. *J Chem Phys* 1940, 8, 812.
16. Avrami, M. J. *J Chem Phys* 1941, 9, 117.
17. Hay, J. N.; Perzekop, Z. J. *J Polym Sci Part B: Polym Phys* 1978, 16, 81.
18. Hay, J. N.; Mills, P. J. *Polymer* 1982, 23, 1380.
19. Rabesiaka, J.; Kovacs, A. J. *J Appl Phys* 1961, 32, 2314.
20. Rana, S. K. *J Appl Polym Sci* 1996, 61, 951.
21. Razavi-Nouri, M.; Hay, J. N. *Polymer* 2001, 42, 8621.
22. Kuo, S. W.; Huang, W. J.; Huang, S. B.; Kao, H. C.; Chang, F. C. *Polymer* 2003, 44, 7709.
23. Carrado, K.; Xu, A. L. *Chem Mater* 1998, 10, 1440.
24. Elah, A. A.; Moet, A. *J Mater Sci* 1996, 31, 3589.
25. Kamal, M. R.; Chu, E. *Polym Eng Sci* 1983, 23, 27.
26. Fornes, T. D.; Paul, D. R. *Polymer* 2003, 44, 3945.
27. Joshi, M.; Butola, B. S.; Simon, G.; Kukaleva, N. *Macromolecules* 2006, 39, 1839.